Thermal conductivity and Seebeck coefficient of $12CaO \cdot 7Al_2O_3$ electride with a cage structure

Sung Wng Kim,[1,*] Ryuichi Tarumi,[2] Hideo Iwasaki,[3] Hiromichi Ohta,[4] Masahiro Hirano,[1] and Hideo Hosono[1,5]

[1]*Frontier Research Center, Tokyo Institute of Technology, Mail Box S2-13, 4259 Nagatsuta, Midori-ku, Yokohama 226-8503, Japan*

[2]*Department of Mechanical Engineering, Graduate School of Engineering, Osaka University, 2-1 Yamadaoka, Suita, Osaka 565-0871, Japan*

[3]*School of Materials Science, JAIST, 1-1 Asahidai, Nomi, Ishikawa 923-1292, Japan*

[4]*Graduate School of Engineering, Nagoya University, Furo-cho, Chikusa, Nagoya 464-8603, Japan*

[5]*Materials and Structures Laboratory, Tokyo Institute of Technology, Mail Box R3-4, 4259 Nagatsuta, Midori-ku, Yokohama 226-8503, Japan*

(Received 1 May 2009; published 4 August 2009)

Thermal conductivity (κ) and Seebeck coefficient (α) of electron-doped light-metal oxide $12CaO \cdot 7Al_2O_3$ (C12A7 electride) with a subnanometer-sized cage structure are reported on single crystals with various electron concentrations (N_e). The semiconducting C12A7 electride exhibits *n*-type conduction with the highest α value of -100 $\mu V\ K^{-1}$ at 300 K. The κ exhibits an amorphouslike T^2 dependence at low temperatures and varies between 2.3 and 4.5 $Wm^{-1}\ K^{-1}$ at 300 K. This is an order-of-magnitude lower than that of the constituents, CaO (15 $Wm^{-1}\ K^{-1}$) and Al_2O_3 (30 $Wm^{-1}\ K^{-1}$). These properties are attributed to the cage structure, suggesting that the semiconducting electride should be regarded as a phonon glass and electron crystal material. The thermoelectric performance of electrides evaluated by a dimensionless figure of merit (ZT) shows an optimized value of 2×10^{-3} at 300 K for the semiconducting electride with N_e of 5×10^{20} cm^{-3}.

DOI: 10.1103/PhysRevB.80.075201 PACS number(s): 72.20.Pa, 62.65.+k, 66.70.−f

I. INTRODUCTION

The phonon glass and electron crystal (PGEC) (Ref. 1) concept proposed by Slack has significantly improved the strategy of material design in thermoelectrics. This class of materials possesses good electrical properties associated with regular atomic configurations and a low thermal conductivity associated with amorphous nature, leading to a high dimensionless figure of merit $ZT = \alpha^2\sigma/\kappa$, where α is the Seebeck coefficient, σ is the electrical conductivity, and κ is the thermal conductivity, of approximately unity.[2] PGEC semiconductors such as skutterudites[3] and Ge clathrates[4] have a common feature in their crystal structure—a nanocage with a large unit cell composed of heavy metal elements—which is a prerequisite for low lattice thermal conductivity (κ_{lat}).[5]

The discovery of the layer-structured cobalt oxide Na_xCoO_2 as a promising candidate for *p*-type thermoelectric material[6] has evoked renewed interest in oxides because of their potential advantages over heavy metal-based materials such as Bi_2Te_3, especially in high-temperature operation, nontoxicity, high oxidation resistance, and high thermal stability. Thus, intensive efforts have been devoted to exploring oxides with a large ZT. These efforts led to the discovery of *n*-type thermoelectric oxides: a $SrTiO_3$ perovskite[7,8] and its derivatives with a natural superlattice structure.[9,10] In particular, two-dimensional electron-gas (2DEG) systems using $SrTiO_3$ and TiO_2 showed a high potential with a ZT of 2.4 at room temperature.[11] However, although light-metal oxides are environmentally benign and naturally abundant, few efforts have been devoted to this oxide group due to its electrical insulating property and high thermal conductivity. These undesirable properties arise from the low mass of constituent atoms and the high vibration frequency of chemical bonds associated with O^{2-} ions.

$12CaO \cdot 7Al_2O_3$ (C12A7),[12] which is composed of only light-metal elements, can be regarded as a clathrate compound due to its three dimensionally connected subnanometer-sized cage structure (Fig. 1). Furthermore, electrical conductivity can be imparted to C12A7 by replacing "free oxygen ions" trapped in the cages with electrons as counter anions. From a chemical viewpoint, the electron-doped C12A7 ($C12A7:e^-$) is considered as an "electride"[13] in which electrons behave as anions, forming the ionic bonds with the molecular framework. The $C12A7:e^-$ electride undergoes a persistent insulator-semiconductor, metal-insulator, and metal-superconductor transitions as electron concentration (N_e) is increased.[14–16] Because of controllability in the electrical conductivity (σ) and a unique cage structure, which has a potential to show a low κ_{lat} value, one may expect the light-metal oxide C12A7 electride to be a PGEC material and a good candidate for thermoelectric material.

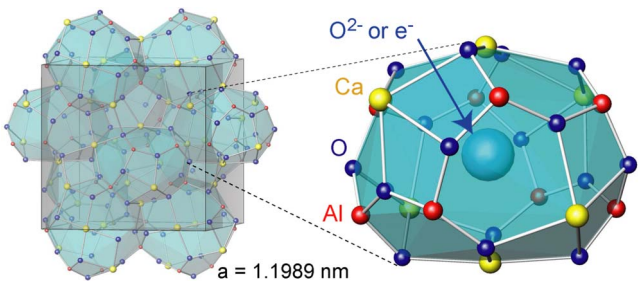

FIG. 1. (Color online) The crystal structure of $12CaO \cdot 7Al_2O_3$. The gray frame indicates a cubic unit cell with the lattice constant of 1.199 nm. The lattice framework, $[Ca_{24}Al_{28}O_{64}]^{4+}$, are positively charged and are composed of 12 cages. Each cage has a free space with ~0.4 nm inner diameter. Two free oxygen ions ($2O^{2-}$) are incorporated as counter anions in two of the 12 cages for maintaining charge neutrality in a unit cell. When each free oxygen ion is replaced by two electrons, electron occupancy in the cage is 4/12.

In this work, we examine the intrinsic thermoelectric transport properties including α and κ of single-crystal C12A7:e^- electrides with various N_e. We find that thermal conductivity at low temperatures is amorphouslike and ZT values reach an optimum value of 2×10^{-3} at N_e of 5×10^{20} cm^{-3}.

II. EXPERIMENTAL DETAILS

Single crystalline C12A7:e^- electrides were prepared by chemical reduction treatments. The details of the synthetic processes were described in an earlier paper.[15] The N_e values of the single-crystal electrides were estimated from optical reflectance spectra in the infrared to ultraviolet region (450–40000 cm^{-1}), measured at 300 K.[17] The transport parameters were measured in the temperature range from 2 to 300 K using a physical property measurement system (Quantum Design). The electrical conductivity (σ) was measured by the four-probe method using Pt electrodes. Seebeck coefficients (α) were measured by alternately heating each end of the sample to create a temperature difference below 1 K. The voltage induced in the sample by the temperature gradient was measured with Chromel/Au-0.07%Fe thermocouples (Nilaco Co.) attached at both ends of sample with a correction for the α of Chromel. The thermal conductivity (κ) was measured by a conventional steady-state method. The acoustic properties were investigated by ultrasound spectroscopy measurement as described in Ref. 18.

III. RESULTS AND DISCUSSION

A. Electrical conductivity and Seebeck coefficient

Figure 2(a) shows the temperature dependence of σ for single-crystal C12A7:e^- electrides in the log-log scale with various N_e. The $\sigma-T$ curves are classified into three types according to their conducting mechanisms: (i) nondegenerated semiconducting (A and B) with $N_e\sim10^{20}$ cm^{-3}, (ii) degenerated semiconducting (C and D) with $5\times10^{20}<N_e<1\times10^{21}$ cm^{-3}, and (iii) metallic (E and F) with $N_e>1\times10^{21}$ cm^{-3}. Electronic transport properties with various N_e are summarized in Table I. In samples A and B, the σ values increase with temperature (positive gradient) in the whole temperature range, showing a thermally activated conduction with $T^{-1/4}$ dependence, presumably via the variable-range-hopping (VRH). The σ values of degenerated semiconductors show a small positive temperature dependence at around RT and are almost constant at low temperatures. Such a behavior is attributed to the coexistence of localization and delocalization of encaged electrons.[17] With a further increase in N_e, the slopes become negative, indicating that the conduction becomes metallic.

Figure 3(a) shows the temperature dependence of α for single-crystal C12A7:e^- electrides with various N_e. The α values of the semiconducting samples (A–D) are negative in a wide temperature range from 20 to 300 K. The highest value of $|\alpha|$ was ~100 μV K^{-1} at 300 K for sample A with N_e of 1×10^{20} cm^{-3} and the value of $|\alpha|$ at 300 K decreases with an increase in N_e. For a VRH semiconductor, α obeys a $T^{1/2}$ dependence.[19] The observed $T^{-1/4}$ dependence of $\sigma(T)$ and the $T^{1/2}$ dependence of $\alpha(T)$ in samples A and B shown in Fig. 3(b) confirms the VRH conduction in these samples.

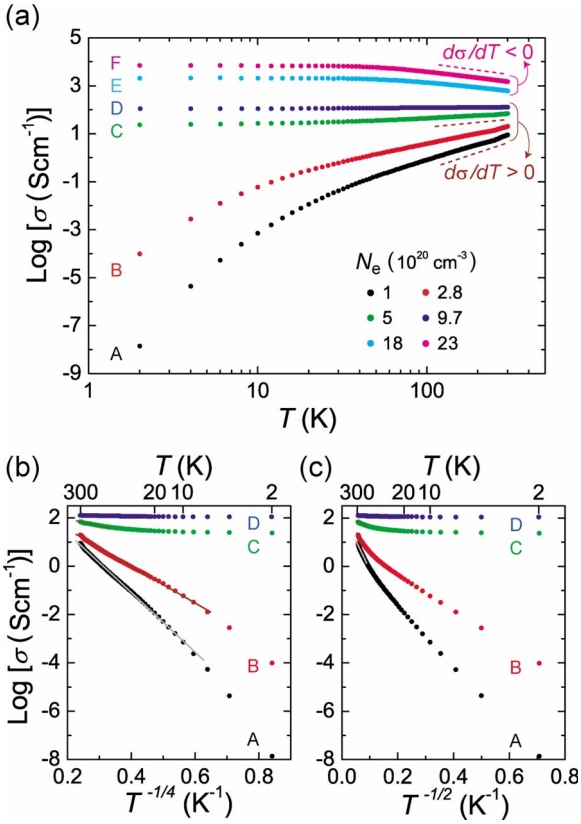

FIG. 2. (Color online) (a) Temperature dependence of electrical conductivity (σ) for single-crystal C12A7:e^- electrides in the log-log scale with various N_e. Samples A–D are semiconducting with $d\sigma/dT>0$, and samples E and F are metallic conducting with $d\sigma/dT<0$. The metal-insulator transition occurs at $N_c\sim1\times10^{21}$ cm^{-3} just above the N_e in sample D. (b) and (c) show that log σ is proportional not to $1/T^{1/2}$ but to $1/T^{1/4}$ over a wide temperature range, implying that conduction is controlled via a three-dimensional variable-range-hopping mechanism without electron-electron interactions.

As N_e increases, the temperature dependence of α becomes closer to a straight line and finally α of sample D in

TABLE I. Electronic transport properties for single-crystal C12A7:e^- electrides at room temperature. Electrical conductivity (σ), Seebeck coefficient (α), mobility (μ), and carrier effective mass (m^*).

Sample	N_e (10^{20} cm^{-3})	σ (S cm^{-1})	α (μV K^{-1})	μ (cm^2 V^{-1} s^{-1})	m^* (m_0)
A	1	9	−90	0.41	
B	2.8	20	−70	0.43	
C	5	68	−50	0.81	1.5
D	9.7	127	−23	0.82	1.1
E	18	613	8	2.13	
F	23	1486	10	4.11	0.82[a]

[a]The value obtained through reflectance-spectra analysis (Ref. 17).

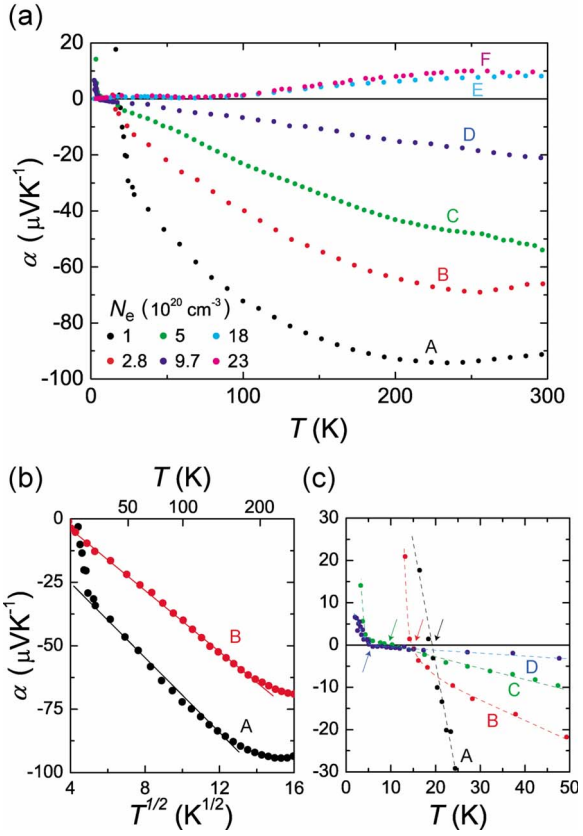

FIG. 3. (Color online) (a) Temperature dependence of Seebeck coefficient (α) for single-crystal C12A7:e$^-$ electrides with various N_e. The sign of α changes from negative on the semiconducting side to positive on the metallic side. (b) The $T^{1/2}$ dependence of α demonstrates that the conduction is controlled via a variable-range-hopping mechanism. (c) Enlarged low temperature regime for samples A–D. Lines are drawn as a guide for the eyes.

the vicinity of metal-insulator transition (MIT) shows an almost linear behavior, which is typical of a metal. If there are two components which affect $\alpha(T)$, i.e., semiconducting (localized states) and metallic (delocalized states) contributions, $\alpha(T)$ should be dominated by the metallic contribution. This is due to the exponential decrease in conductance of semiconducting components with decreasing temperature. Thus, the linear temperature dependence of α in samples C and D originates from the occurrence of the electron delocalization below the MIT in sample C with N_e of 5×10^{20} cm^{-3}. This consideration is compatible with the result obtained through reflectance-spectra analysis,[17] which clarified the coexistence of localized and delocalized electrons for the same N_e. In addition, the metallic conducting samples E and F exhibit positive α values below 10 μV K^{-1} in the whole temperature range.

Degenerated semiconducting samples C and D show rather lower α values than that ($\sim$300 μV K^{-1}) of heavily Nd-doped $SrTiO_3$ single-crystal (degenerated semiconducting).[20] The reason for this observation may be understood as follows: The α of degenerated semiconductors can be expressed by Eqs. (1) and (2)

$$\alpha = \pm \frac{k_B}{e}\left[\frac{2F_1(\eta^*)}{F_0(\eta^*)} - \eta^*\right], \tag{1}$$

$$F_n = \int_0^\infty \frac{x^n}{1+\exp(x-\eta^*)}dx, \tag{2}$$

where η^* is the reduced Fermi level, k_B is the Boltzmann constant, and F_n is the Fermi-Dirac integral of order x. These equations are based on the assumption of one parabolic conduction-band model with acoustic phonon scattering as a dominant carrier-scattering mechanism.[21]

Then, the N_e is given by

$$N_e = 4\pi\left(\frac{2m^*k_BT}{h^2}\right)^{3/2}F_{1/2}(\eta^*), \tag{3}$$

where h, T, and m^* are the Planck constant, absolute temperature, and density-of-states effective mass, respectively. Using the η^* calculated by Eq. (1) from the measured value of α, we evaluated the m^* from Eq. (3) for degenerated semiconducting samples C and D. The results are summarized in Table I. The value of m^* ($1.1-1.5m_0$) for the degenerated C12A7:e$^-$ is rather lower than that ($m^*=7.3-7.7m_0$) (Ref. 20) of the Nd-doped $SrTiO_3$. This difference originates from the nature of conduction-band bottom between them. The former has s-band nature leading to a wide bandwidth while the latter has d-band nature leading to a narrow band.

The value of α in all semiconducting C12A7:e$^-$ samples changes from negative to positive as temperature decreases as shown in Fig. 3(c). The temperature intercept at zero α ($T_{\alpha=0}$) decreases with an increase in N_e. This sign change in $\alpha(T)$ is a common feature of uncompensated semiconductors, such as phosphorus-doped Si, at low temperatures where impurity band conduction is predominant.[22–24] Monotonically increasing α without a maximum below $T_{\alpha=0}$ probably arises from the activation of carriers with a T^{-1} dependence.[23]

B. Thermal conductivity and dimensionless figure of merit, *ZT*

Figure 4 shows the temperature dependence of thermal conductivity (κ) of single-crystal C12A7:O^{2-} (insulating) and C12A7:e$^-$ electride (metallic sample F) in the log-log scale. The single-crystal κ value is 2.3 Wm^{-1} K^{-1} for C12A7:O^{2-} and 4.5 Wm^{-1} K^{-1} for C12A7:e$^-$ at 300 K. These values are an order-of-magnitude lower than those of the constituent oxides, CaO (15 Wm^{-1} K^{-1}) and Al_2O_3 (30 Wm^{-1} K^{-1}). Moreover, these values are lower than those of thermoelectric oxides such as the single-crystal $SrTiO_3$ ($\sim$11 Wm^{-1} K^{-1}) (Ref. 7) and Na_xCoO_2 (10–20 Wm^{-1} K^{-1}).[25,26]

The lattice thermal conductivity (κ_{lat}) of the C12A7:e$^-$ electride is calculated as follows. The total thermal conductivity (κ_{tot}) is the sum of an electronic contribution (κ_{ele}) and a lattice contribution (κ_{lat}). The κ_{ele} can be calculated using the Wiedemann-Franz relation

$$\kappa_{ele} = L_0 \cdot \sigma \cdot T, \tag{4}$$

where L_0 is Lorentz number, σ is electrical conductivity, and T is absolute temperature. For metallic C12A7:e$^-$ (samples

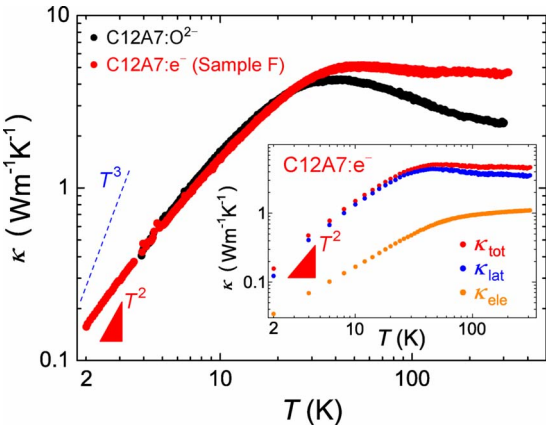

FIG. 4. (Color online) Temperature dependence of thermal conductivity (κ) for single-crystal C12A7:O^{2-} insulator and C12A7:e^- electride metal (Sample F) in the log-log scale. The dashed line at low temperature is T^3, which is typical for crystalline materials. Data for C12A7 follow a T^2 dependence observed in amorphous materials, indicating amorphouslike nature of thermal conduction in a single crystalline C12A7 irrespective of encaged species. Inset shows the electronic and lattice contribution of thermal conductivity of the C12A7:e^- electride in the log-log scale.

E and F), we used a universal Lorentz number of 2.45×10^{-8} V^2 K^{-2} ($=\pi^2 k_B^2/3e^2$). On the other hand, the Lorentz number for degenerated semiconducting C12A7:e^- (samples C and D) can be expressed by Eq. (5) (Ref. 20),

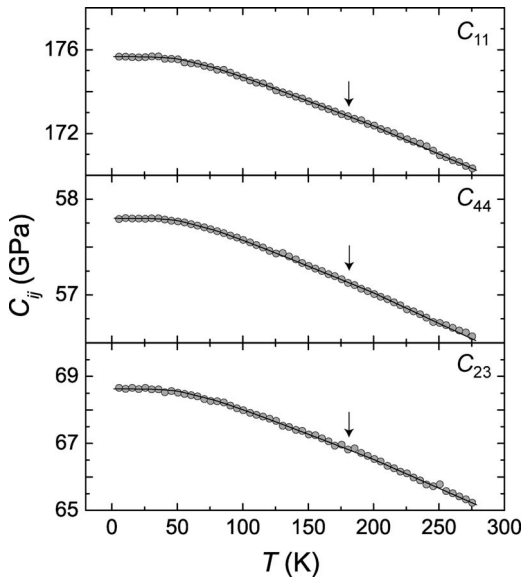

FIG. 5. Temperature dependence of elastic constants (C_{ij}) for single-crystal C12A7:O^{2-}. Open circles are numerically calculated values using observed vibration resonance spectra; solid lines are the least-squares fit using Varshni's function. Arrows show the Einstein temperature, $\Theta_E \sim 180$ K. The same Θ_E in all C_{ij} indicates the phonon modes are isotopic in all crystallographic directions, confirming amorphouslike thermal conductivity of C12A7.

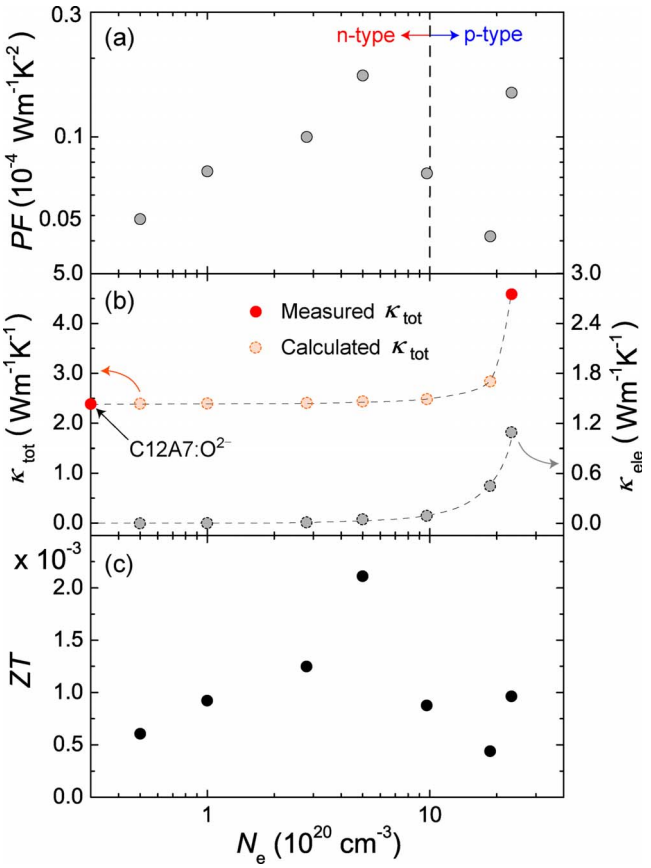

FIG. 6. (Color online) N_e dependence of thermoelectric transport properties for single-crystal C12A7:e^- electrides at 300 K. The X axis is in logarithmic scale for clarity. (a) PF in the log-log scale. (b) Thermal conductivity. Red and gray circles show the measured thermal conductivity and the calculated electronic thermal conductivity, respectively. The electronic thermal conductivity (κ_{ele}) is calculated using Wiedemann-Franz relation with a universal Lorentz number for metallic C12A7:e^- (samples E and F) and Lorentz numbers calculated for degenerated semiconducting C12A7:e^- (samples C and D) using Eq. (5). The κ_{ele} of semiconducting C12A7:e^- showing a VRH-type conduction (samples A and B) is also calculated using Eqs. (1)–(5) for simplicity and the calculated values were negligibly small (<0.5%) compared to the κ_{tot} of C12A7:O^{2-} insulator. Orange circles show the calculated κ_{tot}, on the assumption that the κ_{lat} of C12A7:e^- electrides is the same as that of the C12A7:O^{2-} insulator. (c) The dimensionless figure of merit, ZT, reveals that the optimum N_e for the thermoelectric properties is 5×10^{20} cm^{-3} of a degenerated semiconductor.

$$L_0 = \frac{k_B^2}{e^2} \frac{3F_0(\eta^*) \cdot F_2(\eta^*) - 4F_1^2(\eta^*)}{F_0^2(\eta^*)}. \quad (5)$$

Here, η^* can be calculated from observed values of α using Eqs. (1) and (2).

Inset of Fig. 4 shows calculated κ_{lat} for metallic C12A7:e^- (sample F) as a function of temperature in the log-log scale. Since the calculated value of low temperature $\kappa_{ele}(T)$ of metallic C12A7:e^- (sample F) is negligibly small, indicating that the thermal conduction is mainly due to lattice phonons, it is noted that the low temperature $\kappa(T)$ of

C12A7:e^- electride is almost the same as the low temperature $\kappa_{lat}(T)$. Thus, we may conclude that the low temperature $\kappa_{lat}(T)$ of the metallic C12A7:e^- electride is basically the same as the low temperature $\kappa(T)$ of insulating C12A7:O^{2-}. However, the difference in κ values around 300 K may be attributed to the difference in cage geometry since each cage in the electride is equivalent due to the delocalization of electrons while the insulator has two types of O^{2-} accommodating and O^{2-}-free cages.

It is worth noting that $\kappa(T)$ for both samples at low temperatures is very close to T^2 dependence, which is typical for amorphous materials and is well described by the broad distribution of phonon scattering in two-level systems.[27] This temperature dependence is distinctly distinguishable from that of conventional crystalline materials with T^3 dependence. Therefore, the observed small κ values and the amorphouslike T^2 dependence may be explained by a model of two-level system. In other words, the subnanometer cage structure of C12A7 plays a dominant role in the thermal transport. This result is consistent with the observation that both insulating and metallic C12A7 show the same amorphouslike T^2 dependence irrespective of their encaged species—localized O^{2-} ions and delocalized electrons. This underscores that the vibrational properties of cage skeletons in C12A7 are crucial. Consequently, the amorphouslike T^2 dependence of $\kappa(T)$ together with the semiconducting electrical properties suggest that C12A7:e^- is a PGEC material.

The amorphouslike thermal transport of C12A7 is also supported by a resonant ultrasound spectroscopy (RUS) measurement. RUS is an ultrasonic technique to determine the complete set of elastic constants (C_{ij}) of a solid by measuring the free-body resonances of the sample. From the numerical calculation of C_{ij} using measured resonance spectra[28] for a single-crystal C12A7:O^{2-} insulator, the acoustic Debye temperature (Θ_D) was obtained to be 602 K, which is in good agreement with that determined from a heat-capacity measurement (604 K).[29] Fig. 5 shows the temperature dependence of elastic constants (C_{ij}) for a single-crystal C12A7:O^{2-} insulator. The analysis of the $C_{ij}-T$ curve gives information about the Einstein temperature (Θ_E) for respective phonon modes. The $C_{ij}(T)$ can be expressed in the following equation, the so-called Varshni's function, which is an empirical expression to describe the elastic constant of a material:[30]

$$C_{ij} = C_{ij}(0) - s/(e^{\Theta_E/T} - 1), \tag{6}$$

where $C_{ij}(0)$ is the elastic constant at 0 K and s is an adjustable fitting parameter representing anharmonicity. The solid lines in Fig. 5 represent least-squares fitting results to experimental data (open circles) by Eq. (6). The obtained Θ_E values are nearly the same (~180 K) for the respective C_{ij}, indicating that the phonon vibration modes are isotropic over all crystallographic directions as for glass states. The value of the phonon mean free path (l_{ph}) obtained from $\kappa_{lat} = (1/3) \cdot C_v \cdot v_{ph} \times l_{ph}$ is 0.7 nm at 300 K. This value is obtained by using the average group velocities (v_{ph}), which is calculated with the measured values of C_{11} and C_{44} using relations of $v_L = (C_{11}/\rho)^{1/2}$ and $v_T = (C_{44}/\rho)^{1/2}$,[31] and specific-heat data[32] for the C12A7:O^{2-} insulator. This small l_{ph} value is close to the separation of neighboring cages, indicating that the phonon migration without scattering is limited to a separation between the nearest neighbor cages. Therefore, the low κ value of C12A7 is attributable to the inherent cage structure.

Finally, we evaluated the thermoelectric performance of C12A7:e^- electrides, the power factor (PF=$\alpha^2\sigma$), and ZT as a function of doped N_e in the logarithmic scale. Figure 6 shows that the optimum N_e for electrical properties is located around 5×10^{20} cm^{-3}. The highest power factor (PF) value ($\sim 2\times10^{-5}$ $Wm^{-1}K^{-2}$) is lower than that ($\sim 2\times10^{-3}$ $Wm^{-1}K^{-2}$) of heavily Nd-doped $SrTiO_3$ single crystal.[7,20] This difference is mainly attributed to the low α value originating from the rather low m^* value of the present system. From the calculation of κ_{tot} for all the electride samples, on the assumption that the κ_{lat} is equivalent to κ of insulating C12A7:O^{2-}, the highest ZT of 2×10^{-3} at 300 K was obtained for sample C with N_e of 5×10^{20} cm^{-3}.

IV. CONCLUSION

We have investigated α and κ of single-crystal C12A7:e^- electrides with various N_e, as well as their thermoelectric performance. The semiconducting C12A7:e^- electride exhibits n-type conduction with the highest α value of -100 $\mu V K^{-1}$ at 300 K. The $\kappa(T)$ of single-crystal C12A7:O^{2-} and C12A7:e^- electride shows the amorphouslike T^2 dependence at low temperatures and a small κ values of 2.3–4.5 $Wm^{-1}K^{-1}$ at 300 K. These thermal properties originate from the isotropic phonon mode of C12A7 framework. Thus, the amorphouslike behavior of $\kappa(T)$ together with the semiconducting electrical transport properties suggests that C12A7:e^- electride is a PGEC material. The optimum ZT value is of 2×10^{-3} at 300 K, which is an order-of-magnitude lower than those of $SrTiO_3$ (0.03) and Na_xCoO_2 (0.07). However, we anticipate that ZT can be enhanced if lower κ_{lat} and higher α and σ are obtained by modifying the lattice framework with heavy-mass elements and encaged species.

*Corresponding author; sw-kim@lucid.msl.titech.ac.jp

[1] G. A. Slack, in *CRC Handbook of Thermoelectrics*, edited by D. M. Rowe (CRC, Boca Raton, FL, 1995), p. 407.
[2] G. J. Snyder and E. S. Toberer, Nature Mater. **7**, 105 (2008).
[3] V. Keppens, D. Mandrus, B. C. Sales, B. C. Chakoumakos, P. Dai, R. Coldea, M. B. Maple, D. A. Gajewski, E. J. Freeman, and S. Bennington, Nature (London) **395**, 876 (1998).
[4] G. S. Nolas, J. L. Cohn, G. A. Slack, and S. B. Schujman, Appl. Phys. Lett. **73**, 178 (1998).
[5] C. B. Vining, Nature Mater. **7**, 765 (2008), and references therein.
[6] I. Terasaki, Y. Sasago, and K. Uchinokura, Phys. Rev. B **56**, R12685 (1997).
[7] S. Ohta, T. Nomura, H. Ohta, M. Hirano, H. Hosono, and K.

Koumoto, Appl. Phys. Lett. **87**, 092108 (2005).
[8] H. Ohta, K. Sugiura, and K. Koumoto, Inorg. Chem. **47**, 8429 (2008).
[9] K. H. Lee, S. W. Kim, H. Ohta, and K. Koumoto, J. Appl. Phys. **100**, 063717 (2006).
[10] K. H. Lee, S. W. Kim, H. Ohta, and K. Koumoto, J. Appl. Phys. **101**, 083707 (2007).
[11] H. Ohta, S. W. Kim, Y. Mune, T. Mizoguchi, K. Nomura, S. Ohta, T. Nomura, Y. Nakanishi, Y. Ikuhara, M. Hirano, H. Hosono, and K. Koumoto, Nature Mater. **6**, 129 (2007).
[12] K. Hayashi, S. Matsuishi, T. Kamiya, M. Hirano, and H. Hosono, Nature (London) **419**, 462 (2002).
[13] J. L. Dye, Science **301**, 607 (2003).
[14] S. Matsuishi, Y. Toda, M. Miyakawa, K. Hayashi, T. Kamiya, M. Hirano, I. Tanaka, and H. Hosono, Science **301**, 626 (2003).
[15] S. W. Kim, S. Matsuishi, T. Nomura, Y. Kubota, M. Takata, K. Hayashi, T. Kamiya, M. Hirano, and H. Hosono, Nano Lett. **7**, 1138 (2007).
[16] M. Miyakawa, S. W. Kim, M. Hirano, Y. Kohama, H. Kawaji, T. Atake, H. Ikegami, K. Kono, and H. Hosono, J. Am. Chem. Soc. **129**, 7270 (2007).
[17] S. Matsuishi, S. W. Kim, T. Kamiya, M. Hirano, and H. Hosono, J. Phys. Chem. C **112**, 4753 (2008).
[18] R. Tarumi, M. Hirao, T. Ichitsubo, E. Matsubara, J. Saida, and H. Kato, Phys. Rev. B **76**, 104206 (2007).
[19] M. J. Burns and P. M. Chaikin, J. Phys. C **18**, L743 (1985).
[20] S. Ohta, T. Nomura, H. Ohta, and K. Koumoto, J. Appl. Phys. **97**, 034106 (2005).
[21] V. L. Fistul, *Heavily Doped Semiconductors* (Plenum, New York, 1969).
[22] T. H. Geballe and G. W. Hull, Phys. Rev. **98**, 940 (1955).
[23] N. F. Mott and E. A. Davis, *Electronic Process in Non-Crystalline Materials* (Clarendon Press, Oxford, 1971), p. 164.
[24] X. Liu, A. Sidorenko, S. Wagner, P. Ziegler, and H. v. Löhneysen, Phys. Rev. Lett. **77**, 3395 (1996).
[25] K. Fujita, T. Mochida, and K. Nakamura, Jpn. J. Appl. Phys., Part 1 **40**, 4644 (2001).
[26] M. Lee, L. Viciu, L. Li, Y. Wang, M. L. Foo, S. Watauchi, R. A. Pascal, Jr., R. J. Cava, and, N. P. Ong, Nature Mater. **5**, 537 (2006).
[27] A. C. Anderson, in *Amorphous Solids, Low-Temperature Properties*, edited by W. A. Phillips (Springer-Verlag, New York, 1981), p. 65.
[28] H. H. Demarest, Jr., J. Acoust. Soc. Am. **49**, 768 (1971).
[29] Y. Kohama, T. Tojo, H. Kawaji, T. Atake, S. Matsuishi, and H. Hosono, Chem. Phys. Lett. **421**, 558 (2006).
[30] Y. P. Varshni, Phys. Rev. B **2**, 3952 (1970).
[31] O. L. Anderson, J. Phys. Chem. Solids **24**, 909 (1963).
[32] Y. Kohama, S. W. Kim, T. Tojo, H. Kawaji, T. Atake, S. Matsuishi, and H. Hosono, Phys. Rev. B **77**, 092505 (2008).